frontiers | Frontiers in Materials

TYPE Original Research
PUBLISHED 06 August 2025
DOI 10.3389/fmats.2025.1643683

OPEN ACCESS

EDITED BY
Jue Li,
Chongqing Jiaotong University, China

REVIEWED BY
Wensheng Wang,
Jilin University, China
Qiang Tang,
Soochow University, China
Yangming Gao,
Liverpool John Moores University,
United Kingdom

*CORRESPONDENCE
Jianwei Xie,
23001030005@csust.edu.cn

RECEIVED 09 June 2025
ACCEPTED 22 July 2025
PUBLISHED 06 August 2025

CITATION
Li C, Tan G, Weng H, Shi J, Li S and Xie J (2025) Feasibility of using FA and GGBS-derived geopolymer for high liquid limit soil stabilization.
Front. Mater. 12:1643683.
doi: 10.3389/fmats.2025.1643683

Feasibility of using FA and GGBS-derived geopolymer for high liquid limit soil stabilization

Chenchen Li[1,2], Guohao Tan[2], Hui Weng[1], Jiachen Shi[1], Shixiang Li[1] and Jianwei Xie[2]*

[1]Zhejiang Communications Investment Group Expressway Construction and Management Co., Ltd., Hangzhou, China, [2]National Engineering Research Center of Highway Maintenance Technology, Changsha University of Science & Technology, Changsha, China

Introduction: To improve the comprehensive utilization rate of industrial solid wastes, this study developed geopolymer materials using fly ash ground granulated blast furnace slag (GGBS), sodium silicate, and sodium hydroxide for the stabilization of high liquid limit soil.

Method: A series of tests including compaction, unconfined compressive strength (UCS), California bearing ratio (CBR), resilient modulus, scanning electron microscopy (SEM), and energy dispersive spectroscopy (EDS) were conducted. The investigation focused on the influence of alkali activator modulus and dosage on the strength of geopolymers. Additionally, the impact of geopolymer dosage on the optimum moisture content (OMC), maximum dry density (MDD), UCS, CBR, and resilient modulus of stabilized soil was examined.

Results and discussion: The results indicated that the OMC of the stabilized soil decreased while the MDD increased with increasing geopolymer dosage. The UCS of the stabilized soil significantly improved with the addition of geopolymer, achieving values of 0.52 MPa, 1.68 MPa, 3.25 MPa, and 4.18 MPa at 7 days for geopolymer dosages of 0%, 4%, 8%, and 12%, respectively. Similarly, the CBR of the stabilized soil increased with geopolymer dosage, reaching 1.2%, 3.5%, 6.5%, and 10.5% after 4 days of water immersion for geopolymer dosages of 0%, 4%, 8%, and 12%, respectively. Increasing geopolymer dosage effectively improved the resilient modulus of stabilized soil, but did not affect the stress-dependent behavior of stabilized soil. Increasing confining pressure or decreasing deviatoric stress still resulted in a higher resilient modulus for geopolymer stabilized soil.

KEYWORDS

geopolymer, industrial solid waste, soil stabilization, mechanical properties, subgrade

1 Introduction

China's accelerated industrialization has precipitated an exponential growth in industrial solid waste generation, emerging as a critical environmental challenge. Recent inventories indicate the national stockpile has surpassed 62 billion metric tons, yet alarmingly, less than 40% undergoes systematic recycling (Yang et al., 2021). Predominant disposal methods involving crude landfilling or open-air stockpiling in peri-urban areas have resulted in severe ecosystem degradation coupled with substantial resource depletion. In alignment with the nation's sustainability agenda, the government has formulated ambitious policy directives emphasizing

"advanced technological innovations for high-value-added applications," targeting a 60% utilization rate elevation. This paradigm shift underscores the pressing necessity to develop innovative valorization technologies for circular economy implementation.

High liquid limit soil, a problematic soil type widely distributed throughout the middle-lower Yangtze River basin and northern China, exhibits distinctive geotechnical characteristics including elevated liquid limit values, pronounced plasticity indices, and excessive natural moisture content. When employed as subgrade filler material, its application in subgrade construction often results in excessive deformations, compromised stability, construction complexity, and subgrade-related pathologies (Wang et al., 2017; Stavridakis, 1999; Lu et al., 2019). Consequently, this challenging geomaterial is frequently classified as unsuitable waste in earthwork projects for subgrade construction, as stipulated by the Technical Specifications for Highway Subgrade Design (JTG D30-2015) (JTG, 2015). This regulatory restriction primarily aims to mitigate geotechnical hazards such as differential settlement, slope instability (Jegede, 2000). High liquid limit soil must be improved before it can be used for embankment filling. Among contemporary soil stabilization techniques, chemical amendment using cementitious materials has emerged as the predominant approach (Wang et al., 2012). The cement-mediated stabilization mechanism involves complex physicochemical interactions that yield gels with enhanced binding capacity, superior mechanical strength, and improved hydraulic stability, thereby significantly improving the engineering performance of soil. However, the environmental ramifications of cement production cannot be overlooked. In the traditional production process, manufacturing each ton of cement consumes 1,510 kW h of energy and is associated with approximately 900 kg of CO_2 emissions (Pérez et al., 2024; Shivaprasad et al., 2024). Cumulatively, global cement industry accounts for7% of anthropogenic CO_2 emissions, an environmental burden that escalates concomitantly with rising infrastructure demands (Barbhuiya et al., 2024).

Given the urgent need for energy conservation and emission reduction within the traditional cement industry, coupled with an increasing awareness of ecological protection, numerous scholars are investigating potential alternative cementitious materials. Geopolymers are considered the most promising novel green cementitious materials (Hossain and Akhtar, 2023; Wang et al., 2025). These materials are formed through the reaction of alumino-silicate precursors in a strongly alkaline solution, resulting in a cementitious material characterized by an amorphous three-dimensional network (El Alouani et al., 2024; Almutairi et al., 2021; Li et al., 2022; Shahedan et al., 2024; Pobłocki et al., 2024). Compared to Portland cement, geopolymers exhibit superior mechanical properties and durability (Ren et al., 2024; Song et al., 2024; Zhang, 2024). Utilizing geopolymers for soil stabilization not only reduces the reliance on Portland cement but also achieves enhanced soil mechanical properties. Research has shown that the performance of construction and demolition waste-derived geopolymers is closely related to the chemical composition, reactivity, and particle size characteristics of the precursor materials (Gu et al., 2023; Xie et al., 2025). Xie et al. (2024) proposed a method for stabilizing high liquid limit subgrade soil using geopolymer, an 8% dosage of geopolymer was found to be the most economical option, providing sufficient strength and strain resistance. Sukprasert et al. (2021) formulated a fly ash (FA) and ground granulated blast furnace slag (GGBS)-derived geopolymer for treating silty clay, with its strength increasing as the solidification temperature rose. Chen et al. (2024) observed that at the same water content, as the proportion of geopolymer replacing cement increased, the compressive strength of the stabilized soil first increased and then decreased. Su et al. (2023) found that the strength of cement and geopolymer stabilized organic clay is closely related to matrix compactness, influenced by the quantity of cementitious products and the degree of clay particle cementation. Mozumder and Laskar (2015) studied the strength development patterns of clay stabilized with different geopolymers and found that GGBS-derived geopolymers significantly enhanced the adhesion between clay particles, thereby improving the mechanical, physical, and hydraulic properties of soft clay. Özbay et al. (2016), Song et al. (2000), Qiu et al. (2025) pointed out that the binding effect of geopolymer binders on soil depends on the alkaline environment induced by hydration. To date, most previous studies have focused on the impact of geopolymers on strength improvement in various types of soils such as general soft soil (Abdullah et al., 2021; Zhan et al., 2013), expansive soil (Sahoo and Singh, 2022), sandy soil (Hossein Rafiean et al., 2020), and the stabilization characteristics of contaminated soil (Pu et al., 2022; Gill et al., 2023). Few studies have concentrated on the role of industrial solid waste in the treatment of clay, especially concerning the physical properties and micro-mechanisms of using sustainable geopolymers to stabilized clay. Therefore, it is necessary to systematically evaluate the potential application of GGBS-FA-derived geopolymers in the solidification of organic clay and conduct comprehensive research on their macro-performance and microstructure through a series of mechanical, physical, and microstructural tests.

To address the aforementioned issues, this study aims to develop a method for synthesizing high strength geopolymers using FA and GGBS as raw materials, which is used to stabilize high liquid limit soils. The study analyzed the effects of the modulus and dosage of the alkali activator on the unconfined compressive strength (UCS) of FA-GGBS geopolymers. The optimal mix ratio of FA-GGBS geopolymers was determined. Compaction tests, UCS tests, California bearing ratio (CBR) tests, and resilient modulus tests of geopolymer-stabilized soils were carried out to explore the influence laws of geopolymer dosage and curing conditions on the properties of geopolymer-stabilized soils. In addition, the microscopic mechanism of geopolymer-stabilized soils was investigated through scanning electron microscopy (SEM) and energy-dispersive spectroscopy (EDS) tests (Sahoo and Singh, 2022).

2 Materials and experimental procedures

2.1 Raw materials

The FA utilized in this study was sourced from a coal-fired power plant located in Ninghai, Zhejiang Province. The median particle size (D50) of GGBS and FA were 8.32 μm and 5.88 μm, respectively. X-ray fluorescence (XRF) analysis was performed on

TABLE 1 XRF results of FA (%) and GGBS (%).

Component	SiO_2	CaO	Al_2O_3	Fe_2O_3	K_2O	MgO	TiO_2	Others
FA	50.1	10.5	27.7	5.6	1.5	1.5	1.2	1.9
GGBS	32.2	33.8	16.9	0.4	0.4	11.3	1.5	3.5

TABLE 2 Characteristics of sodium silicate.

Component	SiO_2	Na_2O	H_2O
Weight percentage (%)	27.30%	8.54%	64.16%

both the FA and GGBS, with the results presented in Table 1. The sodium hydroxide employed had a purity exceeding 98.5%, and the initial modulus of sodium silicate (defined as the molar ratio of SiO_2 to Na_2O) was 3.3. Detailed specifications for the sodium silicate are provided in Table 2. Sodium hydroxide and sodium silicate were used in combination as alkaline activators, both of which were procured from professional chemical reagent manufacturers.

The soil utilized in this experiment was collected from the K185 + 000 section of the Yongjinqu expressway in Quzhou, Zhejiang Province. A series of tests were performed on the soil, including compaction, UCS, CBR, and SEM-EDS microscopic analysis. The basic properties of the soil are summarized in Table 3, which classifies the selected material as high liquid limit soil according to the "Specifications for Soil Test in Highway Engineering" (JTG3430-2020). As stipulated in the "Specifications for Subgrade Soil in China" (JTG D30-2015), high liquid limit soils must be treated with inorganic binders prior to their application in subgrade fill.

2.2 Mix design

Under standard curing conditions (20°C ± 2°C, 95% relative humidity), the study investigated the influence of various mixing ratios of precursor materials (FA and GGBS) and the modulus of the alkaline activator on the resulting strength (Liu et al., 2025). Table 4 details the different mixing ratios of the geopolymer curing agent used in this investigation. The experimental design comprised 22 groups, each containing one test sample and two control samples. For each group, the average strength of the three samples was calculated to ensure reliability and consistency of the results (as illustrated in Figures 1, 2). The mixing ratio that produced the highest strength was identified as the Optimum mixing ratio. Which was then used in subsequent experiments.

2.3 Test method

2.3.1 Compaction test

The compaction test was conducted according to the specifications for highway geotechnical testing. Standard compaction tests were performed on stabilized soil with different geopolymer content to determine the OMC and MDD. During the experiment, the stabilized soil was mixed into a standard mold with an internal volume of 956 cm^3. The stabilized soil was compacted into three layers, with each layer receiving 25 evenly distributed blows. A 2.5 kg hammer was used for compaction, and the hammer was freely dropped from a height of 30.5 cm for each blow.

2.3.2 UCS test

The geopolymer and soil were mixed in a concrete mixer at a speed of 22–24 revolutions per minute for a duration of 5 min. Subsequently, alkali activator was introduced into the mixer, and the mixture was further rotated for an additional 3 min to ensure uniformity. The resulting mixture was compacted using a static pressure method to form cylindrical specimens with a diameter of 50 mm and a height of 100 mm, targeting a compaction density of 96%. Prior to conducting the UCS test, the stabilized soil samples were cured under standard conditions (temperature: 20°C ± 2°C, relative humidity: 95%) for periods of 7 days and 28 days. For each condition, three sets of parallel specimens were prepared to ensure reliability and consistency of the results. The strength values reported in the figures represent the average of the strengths obtained from these three sets of parallel specimens.

2.3.3 CBR test

The tests were conducted in accordance with the "Specifications for Geotechnical Testing of Highway Engineering" (JTG3430-2020). For each curing period (7 days and 28 days), three samples were prepared. Light compaction energy was employed to form the geopolymer samples, utilizing the MDD and OMC values determined for the mix design. After placing the samples in molds, they were cured at room temperature. Specifically, the molds were filled in three layers, with each layer receiving 56 hammer blows to ensure uniform compaction. This method facilitated achieving the desired MDD-OMC conditions for each sample, ensuring consistency and reliability in the test results.

2.3.4 Resilient modulus test

The resilient modulus test was carried out by Dynatriax 100/14 dynamic triaxial testing machine, and the loading sequence of the soil was adopted the loading sequence recommended by "Geotechnical Test Specification" (JTG 3430–2020), as shown in Table 5, the loading waveform was half-sine wave, and the loading frequency was 10 Hz, the loading time was 0.1 s, and the interval time was 0.9 s. The size of the specimen was 100 mm × 200 mm cylindrical specimen, and the curing age was 7 days. The moisture content of the specimen was 1.0 OMC, and the degree of compaction was 96%.

TABLE 3 Physical properties of soil.

Liquid limit (%)	Plastic limit (%)	Plasticity index	Specific gravity	OMC (%)	MDD (g/cm^3)
55.3	36.9	18.4	2.71	16.3	1.62

OMC, optimum moisture content, MDD, maximum dry density.

TABLE 4 Mix proportion scheme of geopolymer.

No.	Precursor materials		Activator	Alkali activator dosage	Water- precursor ratio	Curing condition
	FA	GGBS	Modulus			
S1	100	0	1.0	0.30	0.35	20°C ± 2°C 95% relative humidity
S2	100	0	1.0	0.35	0.35	
S3	100	0	1.0	0.40	0.35	
S4	100	0	1.2	0.30	0.35	
S5	100	0	1.2	0.35	0.35	
S6	100	0	1.2	0.40	0.35	
S7	100	0	1.4	0.30	0.35	
S8	100	0	1.4	0.35	0.35	
S9	100	0	1.4	0.40	0.35	
S10	100	0	1.6	0.30	0.35	
S11	100	0	1.6	0.35	0.35	
S12	100	0	1.6	0.40	0.35	
S13	90	10	1.0	0.30	0.35	
S14	90	10	1.0	0.35	0.35	
S15	90	10	1.0	0.40	0.35	
S16	90	10	1.2	0.30	0.35	
S17	90	10	1.2	0.35	0.35	
S18	90	10	1.2	0.40	0.35	
S19	90	10	1.4	0.30	0.35	
S20	90	10	1.4	0.35	0.35	
S21	90	10	1.4	0.40	0.35	
S22	90	10	1.6	0.30	0.35	
S23	90	10	1.6	0.35	0.35	
S24	90	10	1.6	0.40	0.35	

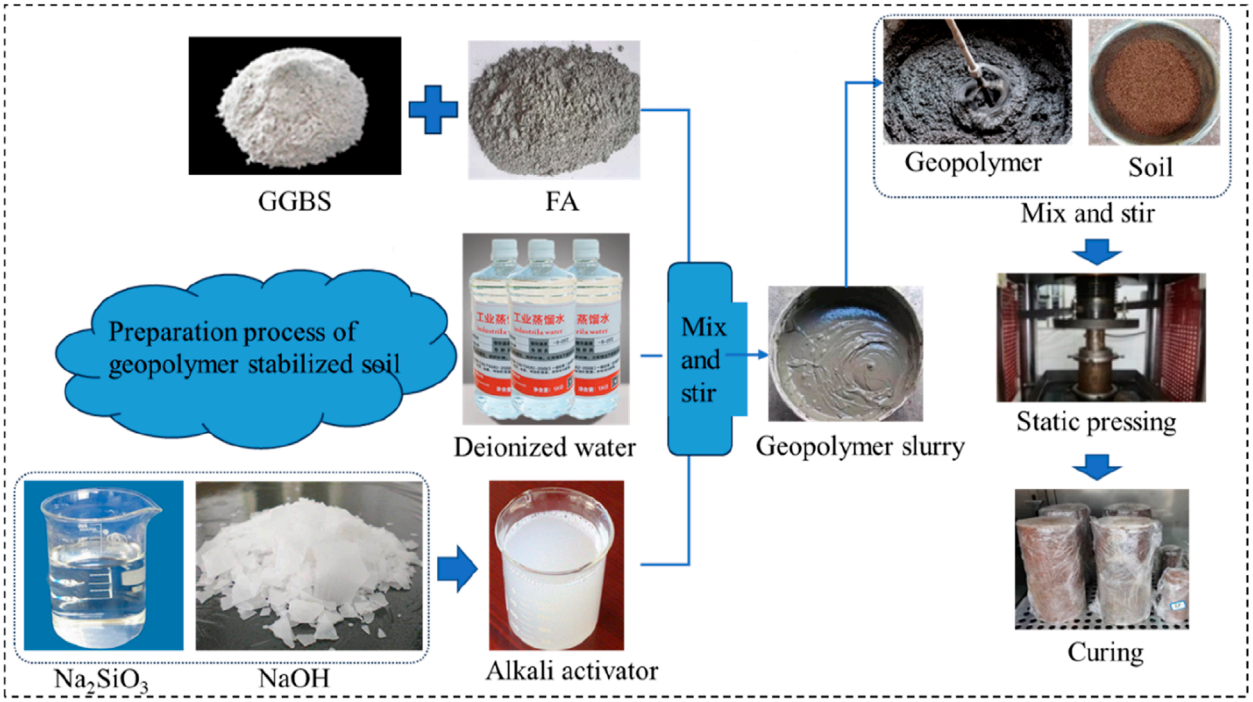

FIGURE 1
Preparation process of geopolymer stabilized soil specimen.

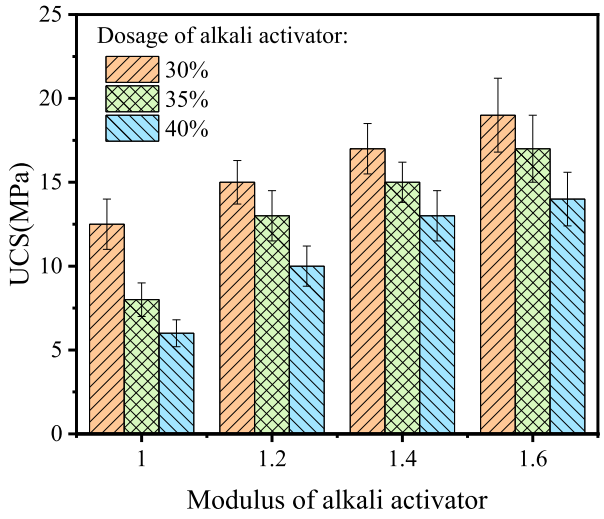

FIGURE 2
UCS of FA based geopolymer.

2.3.5 SEM-EDS microscopic test

In order to study the morphology and chemical properties of geopolymer-stabilized soil, selected soil samples were subjected to SEM and EDS testing. The SEM and EDS tests were performed using a Zeiss EVO-10 scanning electron microscope. EDS testing was conducted on gel points identified from the SEM images, allowing for the determination of the elemental composition of the gel in the geopolymer stabilized soil. The experimental scheme for this study is shown in Figure 1.

3 Results and discussion

3.1 UCS of geopolymer

As shown in Figures 2, 3, the UCS of FA geopolymers did not exceed 20 MPa. However, substituting 10% of the FA with GGBS significantly enhanced the strength. Several factors contributed to this phenomenon: a. GGBS primarily consisted of calcium silicate and calcium aluminate, among other components. These constituents exhibited high reactivity and could chemically interact with the active silica and alumina in FA to form additional geopolymer gels, thereby augmenting the material's strength. b. Particle Characteristics of GGBS: The particles of GGBS were typically very fine, resulting in a large specific surface area. This characteristic increased the contact area between GGBS and reactive geopolymer components, promoting higher reaction rates and enhanced strength development. c. Improved Microstructure: The incorporation of GGBS improved the microstructure of the geopolymer. The formation of gel structures, such as calcium aluminosilicate gel, through the reaction of GGBS within the geopolymer matrix increased the material's density and hardness, thus contributing to higher strength.

The UCS of FA - GGBS based polymer was shown in Figure 3. In the low modulus interval (1.0–1.2), as the modulus increased

10.3389/fmats.2025.1643683

TABLE 5 Loading sequence of soil specimens.

No.	Confining pressure σ_3 (kPa)	Contact stress σ_c (kPa)	Deviatoric stress σ_d (kPa)	Axial stress σ_{max} (kPa)	Number of load cycle times
Preload	30	6	55	61	1,000
1	60	12	30	42	100
2	45	9	30	39	100
3	30	6	30	36	100
4	15	3	30	33	100
5	60	12	55	67	100
6	45	9	55	64	100
7	30	6	55	61	100
8	15	3	55	58	100
9	60	12	75	87	100
10	45	9	75	84	100
11	30	6	75	81	100
12	15	3	75	78	100
13	60	12	105	117	100
14	45	9	105	114	100
15	30	6	105	111	100
16	15	3	105	108	100

from 1.0 to 1.2, the strength enhancement at the same dosage was minimal. For example, the 7-day strength increased from 25 MPa to 27 MPa at a 30% dosage, decreased slightly from 31 MPa to 28 MPa at a 35% dosage, and remained at 28 MPa at a 40% dosage. In the medium - high modulus range (1.4–1.6), as the modulus increased from 1.4 to 1.6, the strength increased significantly. For example, at a 40% dosage, the 7-day strength decreased slightly from 38 MPa to 35 MPa but remained higher than that of the low modulus group; at a 35% dosage, it increased from 29 MPa to 33 MPa. There was a peak phenomenon. At a modulus of 1.4 and a 40% dosage, the strength reached the highest value of 38 MPa, suggesting that the combination of intermediate modulus (1.4) and high dosage was more favorable for strength development. This was because the higher alkali content (Na_2O) at low modulus (1.0–1.2) provided a strong alkaline environment initially, promoting the dissolution of Al_2O_3 and SiO_2 in FA and GGBS. However, the low polymerization degree of SiO_2 resulted in a high concentration of silicate ions, which readily formed a low polymerization gel phase with Al^{3+}, but the structure was loose and the strength enhancement was limited. In the medium-high modulus range (1.4–1.6), the polymerization degree of SiO_2 increased, the alkali content decreased relatively, and the initial dissolution rate slowed down. However, silicate ions readily formed long - chain polymerization structures and three-dimensional network gel phases with Al^{3+} (such as higher polymerization degree N-A-S-H gels), improving structural densification and significantly increasing strength. At a modulus of 1.4, the alkali content and SiO_2 polymerization degree reached a balance, promoting raw material dissolution and stable network structure formation, thus peaking strength at high dosage.

3.2 Compaction curve

The incorporation of FA-GGBS geopolymers showed an inverse relationship with the OMC of high liquid limit soil. This phenomenon could be attributed to the formation of geopolymeric gels when FA-GGBS geopolymers were combined with high liquid limit soil. These gels filled the voids between soil particles, enhancing their bonding strength and compactness, which in turn increased the MDD. Moreover, since geopolymer materials had inherent water absorption capabilities, they effectively reduced the moisture content within the soil by absorbing some of this water. This reduction not only lowered the OMC but

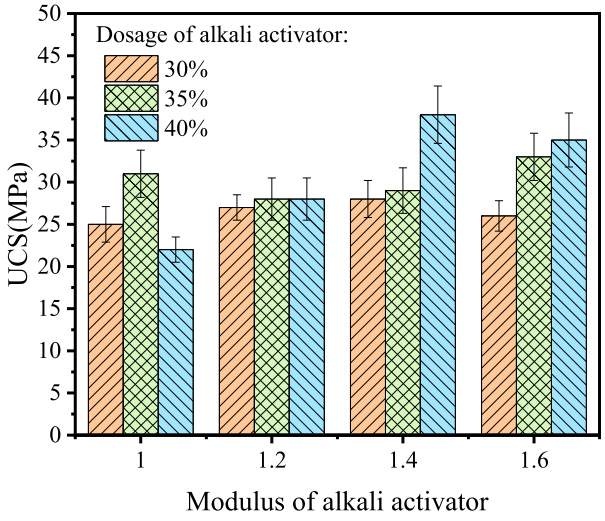

FIGURE 3
UCS of FA -10% GGBS based geopolymer.

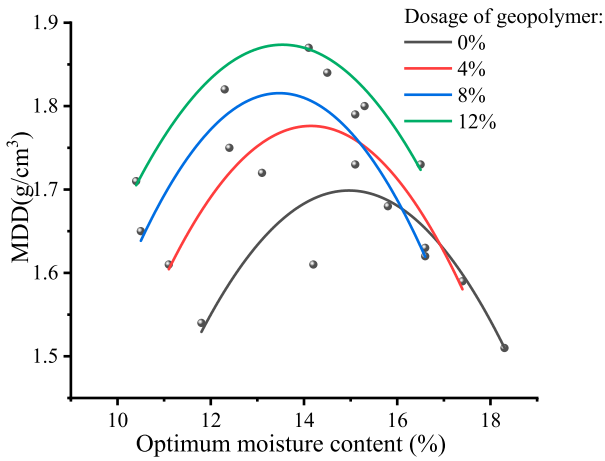

FIGURE 4
Compaction curve of geopolymer stabilized soils.

also decreased the amount of free water between soil particles, facilitating more intimate contact among them. Consequently, these interactions contributed to a higher MDD. The results of the Proctor tests, as shown in Figure 4, demonstrated these effects. Subsequent experiments were carried out at the determined OMC and maximum dry densities corresponding to various geopolymer contents.

3.3 UCS of geopolymer stabilized soils

Figure 5 illustrated the UCS of FA-GGBS geopolymer stabilized soil under various curing temperatures. Under standard curing conditions, the UCS of the stabilized soil at 7 days was higher than that of the geopolymer - stabilized soil cured at 0°C but lower than that cured at 40°C. At high curing temperatures (40°C), the reaction rate of the geopolymer significantly increased, accelerating the formation process and leading to a greater quantity of geopolymer gel being produced in a shorter period. This contributed to achieving higher strength more rapidly. However, excessively high temperatures might have compromised the stability of certain reaction products, potentially resulting in long term structural instability of the gel and affecting its ultimate long term strength performance. Conversely, at low curing temperatures (0°C), the chemical reaction rate of the geopolymer markedly decreased, hindering the hydration and gelation processes. This inhibition led to incomplete reactions between the geopolymer and the soil's raw materials, thereby producing an insufficient amount of gel and negatively impacting strength development. Consequently, the UCS under low temperature curing was lower compared to that under standard curing conditions. These findings emphasized the critical role of curing temperature in influencing the strength development of geopolymer stabilized soils. Understanding these effects provided valuable insights for optimizing curing conditions to achieve desired mechanical properties in practical applications.

At 28 days, the UCS of the stabilized soil under standard curing conditions was the highest, whereas the geopolymer stabilized soil cured at 40°C exhibited greater strength than that cured at 0°C. This observation could be explained as follows: Under standard curing conditions, the geopolymer stabilized soil had achieved full reaction completion and stable hydration products by 28 days, resulting in maximal strength development. In contrast, although the geopolymer stabilized soil cured at high temperature (40°C) exhibited higher strength at 7 days, due to the accelerated reaction rate and increased gel production, its strength dropped below the standard curing conditions at 28 days. This reduction was attributed to potential structural instability caused by high curing temperatures, which might have compromised long term performance. Meanwhile, the geopolymer stabilized soil under low temperature (0°C) curing conditions demonstrated some improvement in strength at 28 days but still recorded the lowest UCS values among the tested conditions.

3.4 CBR

In this study, unsoaked CBR tests and soaked CBR tests (after 4 and 8 days of soaking) were carried out on stabilized soil samples with four different geopolymer contents at both 7 and 28 days of curing. The effects of geopolymer content and soaking duration on the CBR values were analyzed. The results were presented in Figures 6, 7. The findings indicated that as the curing time extended, the CBR values of all stabilized soil samples increased. This enhancement was attributed to the continuous progression of geopolymerization reactions, which strengthened the internal structure of the soil. Conversely, the CBR values of geopolymer stabilized soil significantly decreased with extended soaking periods. This reduction was due to the gradual increase in soil moisture content as soaking time increased. When the soil became fully saturated, pore water pressure rose, leading to a decrease in effective stress within the soil matrix, thus diminishing its bearing capacity. During the soaking process, water penetrated the soil pores, softening the soil and consequently affecting its CBR value. Furthermore, prolonged soaking could induce structural changes

10.3389/fmats.2025.1643683

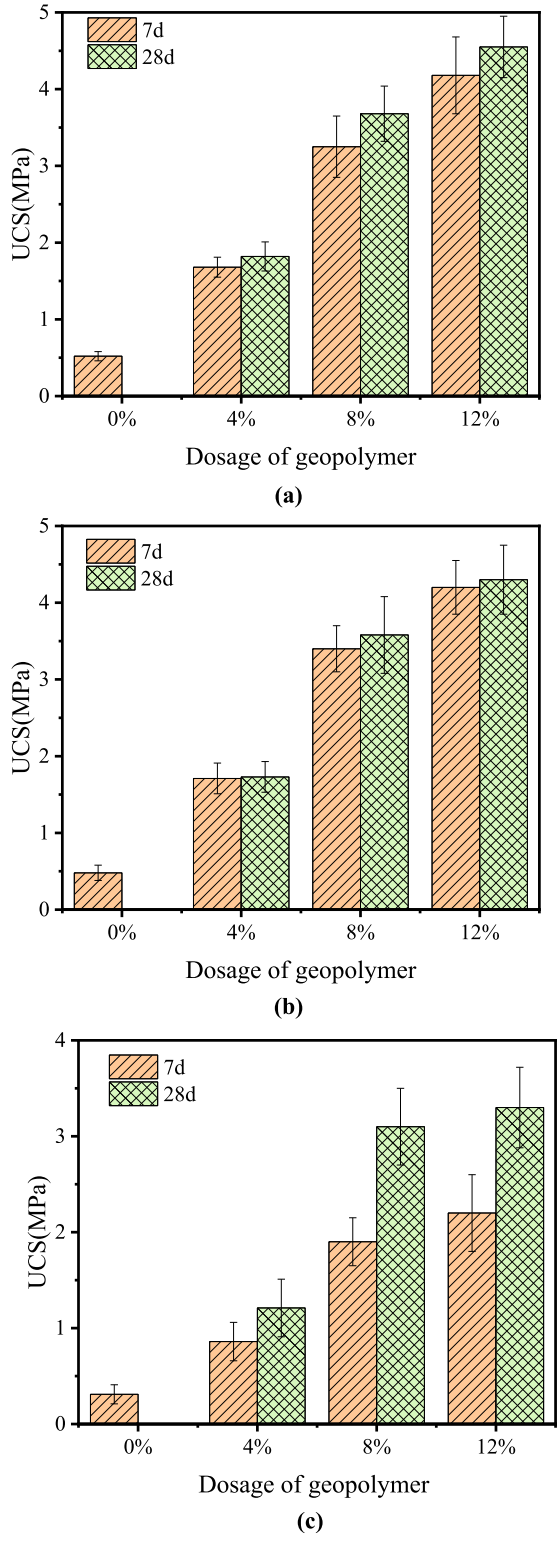

FIGURE 5
UCS of stabilized soil under various curing temperatures. **(a)** Curing at 20°C. **(b)** Curing at 40°C. **(c)** Curing at 0°C.

in the soil, such as weakening the bond between soil particles and altering their relative positions. These alterations resulted in reduced bearing capacity, further contributing to the decline in CBR values.

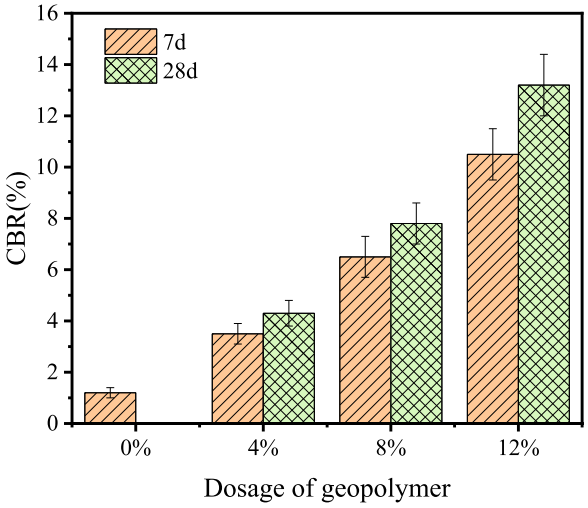

FIGURE 6
CBR value for 4 days of immersion.

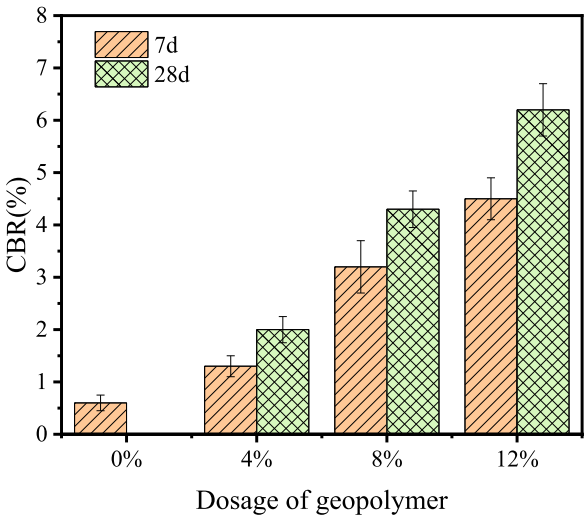

FIGURE 7
CBR value for 8 days of immersion.

3.5 Resilient modulus

Figure 8 shows the resilient modulus trends for geopolymer-stabilized soils under varying stresses. Resilient modulus decreased with rising deviatoric stress at constant confining pressure. For instance, unstabilized soils dropped by 6.34%, 11.15%, and 17.24% as deviatoric stress rose from 30 kPa to 55 kPa, 75 kPa, and 105 kPa. Similarly, geopolymer-treated soils (4%, 8%, 12%) saw declines of 10.11%, 13.21%, and 10.01% under the same stress increments. This occurred because higher deviatoric stress increased vertical deformation, reducing modulus when strain outpaced stress growth. Confining pressure positively influenced modulus. At 30 kPa deviatoric stress, unstabilized soil modulus

10.3389/fmats.2025.1643683

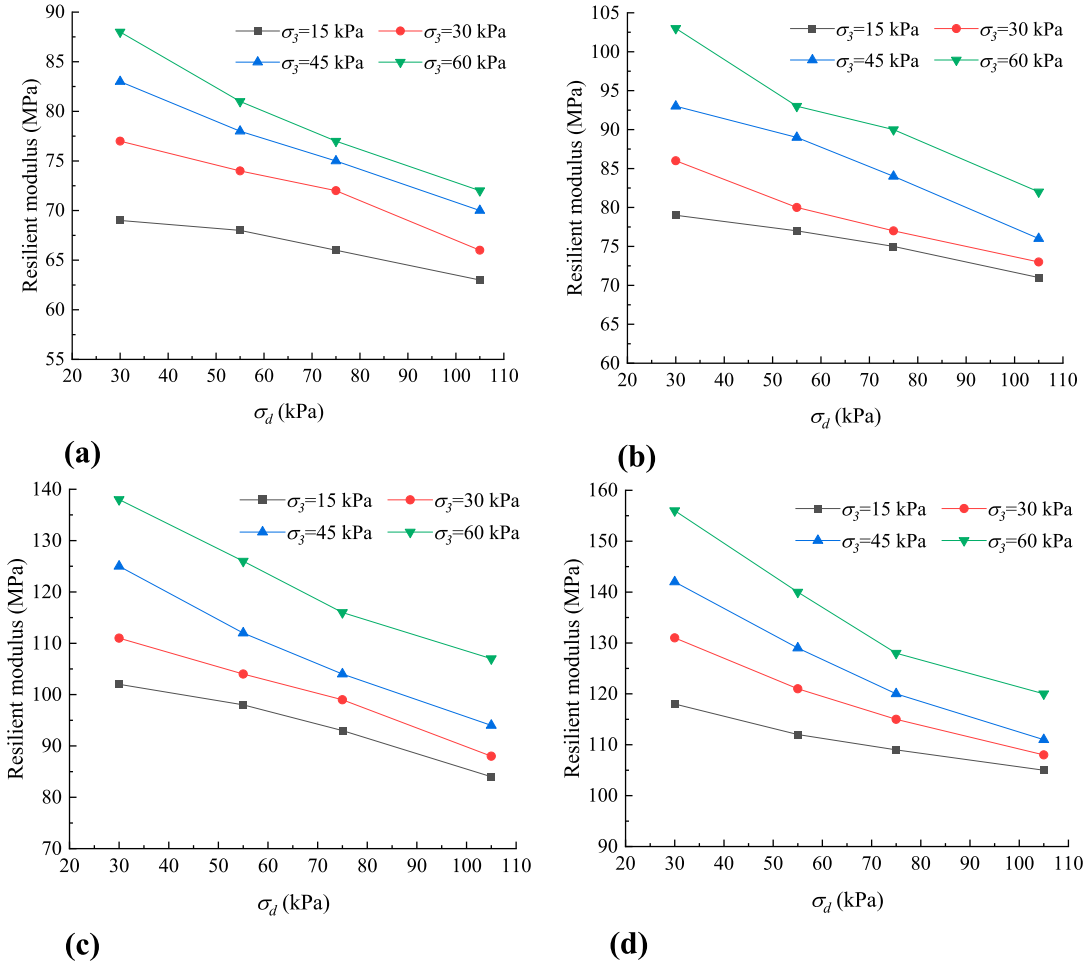

FIGURE 8
Resilient modulus of unstabilized and geopolymer stabilized soils. **(a)** 0% dosage of geopolymer. **(b)** 4% dosage of geopolymer. **(c)** 8% dosage of geopolymer. **(d)** 12% dosage of geopolymer.

rose 12.94%, 21.90%, and 29.36% as confining pressure increased from 15 kPa to 30 kPa, 45 kPa, and 60 kPa. Geopolymer-treated soils (4%, 8%, 12%) showed boosts of 9.69%, 18.68%, and 31.77% under identical pressure changes. Greater lateral confinement from higher confining pressure hardened the soil, enhancing modulus.

Geopolymer dosage significantly impacted modulus. At 60 kPa confining pressure and 30 kPa deviatoric stress, increasing geopolymer from 0% to 4%, 8%, and 12% raised modulus by 17.84%, 56.22%, and 75.13%. The relationship followed a "weak-strong-weak" pattern: modest gains at low dosages (4%), maximum improvement at 8%, and diminishing returns at 12%. This trend is explained by geopolymer gel behavior. Low dosages (4%) produce limited gel, insufficient to fully fill soil voids. As dosage rises to 8%, gel fully occupies voids, strengthening particle bonds and embedding. Beyond 8%, excess gel adds minimal structural benefit, leading to weaker modulus gains. Overall, optimal geopolymer content balances void filling and particle reinforcement to maximize resilient modulus.

3.6 SEM-EDS microscopic test

Figure 9 illustrated the microstructure of unstabilized soil and FA-GGBS geopolymer stabilized soil. The images revealed that the unstabilized soil primarily consisted of solid particles, pores, and internal cracks. After the addition of the FA-GGBS geopolymer, the generated geopolymer gel filled these pores and cracks, effectively binding the solid particles together. It was observed that the stabilized soil with a 4% geopolymer content still showed a considerable number of pores and cracks. However, as the geopolymer content increased, the porosity of the stabilized soil decreased significantly. This reduction in porosity accounted for the higher CBR and UCS values observed in soils stabilized with 8% and 12% FA-GGBS geopolymer compared to those stabilized with 4% geopolymer. This proves that the mechanical properties of stabilized soils are related to microscopic porosity, and as soil porosity decreases, the mechanical properties get improved.

As shown in Figure 10, EDS analysis indicated that the dominant elements within the geopolymer gel were oxygen

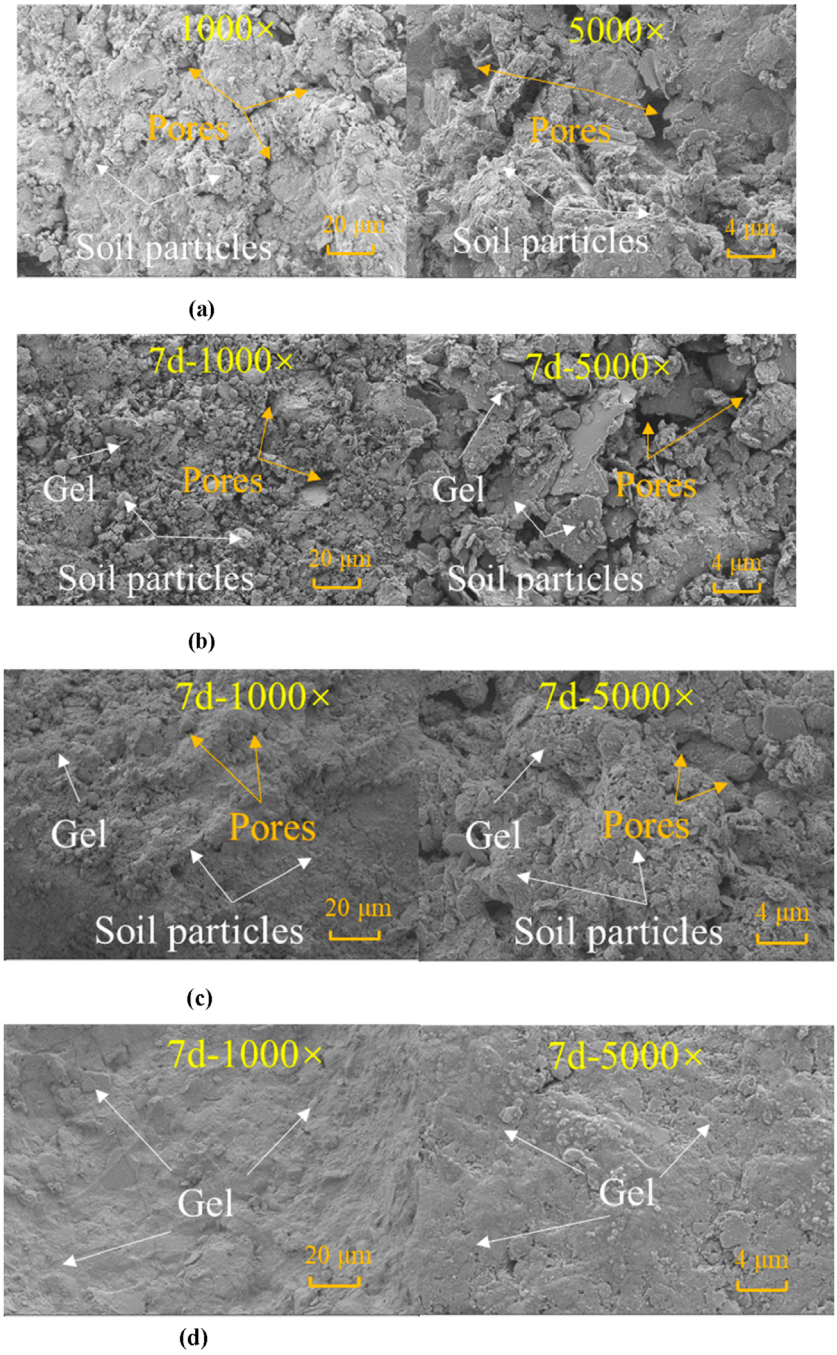

FIGURE 9
SEM of unstabilized and stabilized soils with different geopolymer dosages (after 7 days of curing). **(a)** Stabilized soil with 0% dosage of geopolymer. **(b)** Stabilized soil with 4% dosage of geopolymer. **(c)** Stabilized soil with 8% dosage of geopolymer. **(d)** Stabilized soil with 12% dosage of geopolymer.

(O), silicon (Si), aluminum (Al), calcium (Ca), and sodium (Na). These findings suggested that the primary types of gel formed in FA-GGBS geopolymer stabilized soil were likely to be calcium aluminosilicate hydrates (C-A-S-H) and calcium silicate hydrates (C-S-H). Additionally, sodium aluminosilicate hydrate (N-A-S-H) gel was also present in the geopolymer stabilized soil, which contributed to its enhanced mechanical properties.

4 Conclusion

This study explores the mix design of fly ash (FA) and ground granulated blast furnace slag (GGBS)-based geopolymers and their efficacy in enhancing the properties of high liquid limit soil. A comprehensive series of tests were conducted, encompassing compaction tests, unconfined compressive strength (UCS) tests, California bearing ratio (CBR) tests, resilient modulus tests, and

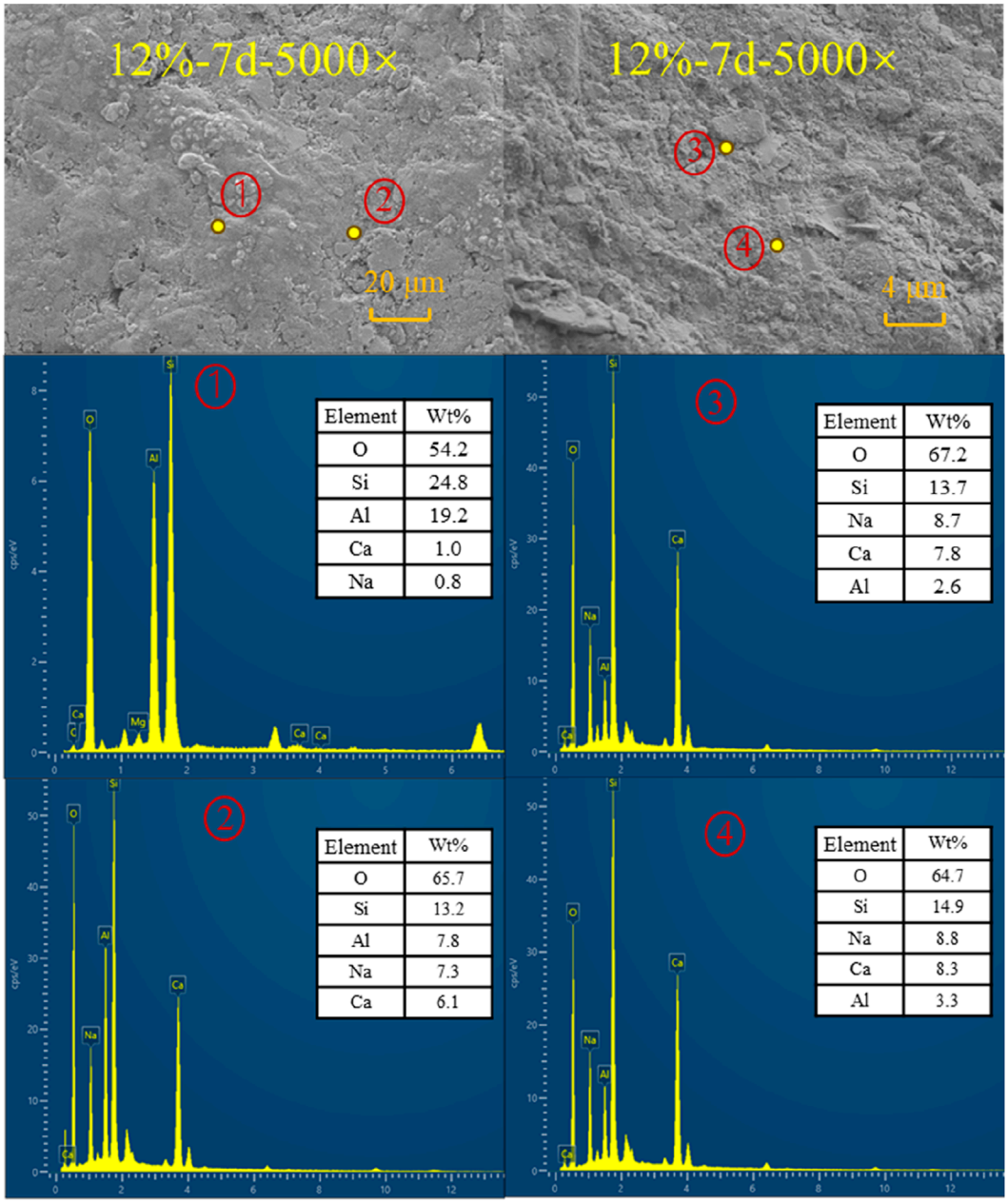

FIGURE 10
EDS test results of 12% geopolymer stabilized soil.

scanning electron microscopy-energy dispersive spectroscopy (SEM-EDS) analysis. The investigation focused on several key factors: the influence of varying proportions of FA and GGBS in the precursor materials, the impact of the modulus of the alkaline activator, and the dosage of the alkaline activator on geopolymer strength. Additionally, the study assessed how different dosages of geopolymer affect the UCS, CBR, and resilient modulus of stabilized soil. Based on the results obtained, the following conclusions can be drawn:

- Compaction tests indicated that the addition of FA-GGBS geopolymers led to an increase in the maximum dry density (MDD) of the soil and a decrease in the optimum moisture content (OMC). These results emphasize the necessity of considering the geopolymer dosage when preparing stabilized soil specimens to minimize experimental errors. This adjustment in compaction parameters suggests that the geopolymer alters the soil's physical structure.

- The UCS test results indicated that FA-GGBS geopolymer stabilized soil achieved strengths of 4.18 MPa after 7 days and 4.55 MPa after 28 days with a 12% geopolymer dosage. These values confirm the suitability of this material for use as highway subgrade soil. According to the CBR test results, the geopolymer-stabilized soil reached a CBR value of 10.5% after 7 days of curing and 13.2% after 28 days. These values exceed the maximum requirement of 8% specified in the "Technical Specification for Construction of Highway Subgrades JTG/T3610-2019″for subgrade soil, highlighting its excellent load bearing capacity and suitability for practical highway construction applications. Increasing the geopolymer dosage effectively improved the resilient modulus of stabilized soil, but did not affect the stress-dependent behavior of stabilized soil. Increasing confining pressure or decreasing deviatoric stress still resulted in a higher resilient modulus for geopolymer stabilized soil.
- SEM - EDS analysis revealed that at a 4% geopolymer content, the stabilized soil had numerous pores and cracks. Nevertheless, increasing the geopolymer content to 8% or 12% significantly reduced the porosity. The generated geopolymer gel filled these pores and cracks, effectively binding the solid particles together. The primary gel types identified in the geopolymer stabilized soil were calcium - aluminosilicate hydrates (C-A-S-H) and calcium silicate hydrates (C-S-H), with sodium - aluminosilicate hydrate (N-A-S-H) also present. These gel formations contribute to the improved mechanical properties of the stabilized soil by providing a cohesive matrix that enhances particle to particle bonding and overall structural integrity.

FA and GGBS-derived geopolymers have the potential to replace cement and lime for road subgrade and subgrade soil stability as well as road grouting. The future research focus will be on the development and application of this geopolymer material in road engineering.

Data availability statement

The original contributions presented in the study are included in the article/supplementary material, further inquiries can be directed to the corresponding author.

Author contributions

CL: Methodology, Writing – original draft, Investigation. GT: Methodology, Writing – review and editing. HW: Methodology, Writing – review and editing, Funding acquisition. JS: Writing – review and editing. SL: Writing – review and editing. JX: Conceptualization, Methodology, Writing – review and editing.

Funding

The author(s) declare that financial support was received for the research and/or publication of this article. The authors acknowledge the financial support of the Major R&D Project of Zhejiang Provincial Department of Transportation (ZJXL-SJT-202316A).

Conflict of interest

Authors CL, HW, JS, and SL were employed by Zhejiang Communications Investment Group Expressway Construction and Management Co., Ltd.

The remaining authors declare that the research was conducted in the absence of any commercial or financial relationships that could be construed as a potential conflict of interest.

Generative AI statement

The author(s) declare that no Generative AI was used in the creation of this manuscript.

Publisher's note

References

Abdullah, H. H., Shahin, M. A., Walske, M. L., and Karrech, A. (2021). Cyclic behaviour of clay stabilised with fly-ash based geopolymer incorporating ground granulated slag. *Transp. Geotech.* 26, 100430. doi:10.1016/j.trgeo.2020.100430

Almutairi, A. L., Tayeh, B. A., Adesina, A., Isleem, H. F., and Zeyad, A. M. (2021). Potential applications of geopolymer concrete in construction: a review. *Case Stud. Constr. Mater.* 15, e00733. doi:10.1016/j.cscm.2021.e00733

Barbhuiya, S., Kanavaris, F., Das, B. B., and Idrees, M. (2024). Decarbonising cement and concrete production: strategies, challenges and pathways for sustainable development. *J. Build. Eng.* 86, 108861. doi:10.1016/j.jobe.2024.108861

Chen, M., Wu, D., Chen, K., Cheng, P., and Tang, Y. (2024). The influence of fly ash-based geopolymer on the mechanical properties of OPC-solidified soil. *Constr. Build. Mater.* 432, 136591. doi:10.1016/j.conbuildmat.2024.136591

El Alouani, M., Saufi, H., Aouan, B., Bassam, R., Alehyen, S., Rachdi, Y., et al. (2024). A comprehensive review of synthesis, characterization, and applications of aluminosilicate materials-based geopolymers. *Environ. Adv.* 16, 100524. doi:10.1016/j.envadv.2024.100524

Gill, P., Jangra, P., Roychand, R., Saberian, M., and Li, J. (2023). Effects of various additives on the crumb rubber integrated geopolymer concrete. *Clean. Mater.* 8, 100181. doi:10.1016/j.clema.2023.100181

Gu, F., Xie, J., Vuye, C., Wu, Y., and Zhang, J. (2023). Synthesis of geopolymer using alkaline activation of building-related construction and demolition wastes. *J. Clean. Prod.* 420, 138335. doi:10.1016/j.jclepro.2023.138335

Hossain, S. S., and Akhtar, F. (2023). Recent progress of geopolymers for carbon dioxide capture, storage and conversion. *J. CO_2 Util.* 78, 102631. doi:10.1016/j.jcou.2023.102631

Hossein Rafiean, A., Najafi Kani, E., and Haddad, A. (2020). Mechanical and durability properties of poorly graded sandy soil stabilized with activated slag. *J. Mater. Civ. Eng.* 32 (1), 04019324. doi:10.1061/(asce)mt.1943-5533.0002990

Jegede, G. (2000). Effect of soil properties on pavement failures along the F209 highway at Ado-Ekiti, south-western Nigeria. *Constr. Build. Mater.* 14 (6-7), 311–315. doi:10.1016/s0950-0618(00)00033-7

JTG (2015). *Specifications for design of highway subgrades*. Wuhan, China: China Communications Second Highway Survey and Design Research Institute Co. Ltd.

Li, X., Bai, C., Qiao, Y., Wang, X., Yang, K., and Colombo, P. (2022). Preparation, properties and applications of fly ash-based porous geopolymers: a review. *J. Clean. Prod.* 359, 132043. doi:10.1016/j.jclepro.2022.132043

Liu, C., Li, Z., and Ye, G. (2025). Mechanisms of efflorescence of alkali-activated slag. *Cem. Concr. Compos.* 155, 105811. doi:10.1016/j.cemconcomp.2024.105811

Lu, Z., Fang, R., Zhan, Y., and Yao, H. (2019). Study on the dynamic deformation of road high liquid limit subgrade soil. *Adv. Civ. Eng.* 2019 (1), 4084983. doi:10.1155/2019/4084983

Mozumder, R. A., and Laskar, A. I. (2015). Prediction of unconfined compressive strength of geopolymer stabilized clayey soil using artificial neural network. *Comput. Geotechnics* 69, 291–300. doi:10.1016/j.compgeo.2015.05.021

Özbay, E., Erdemir, M., and Durmuş, H. İ. (2016). Utilization and efficiency of ground granulated blast furnace slag on concrete properties–A review. *Constr. Build. Mater.* 105, 423–434. doi:10.1016/j.conbuildmat.2015.12.153

Pérez, O. F. A., Arrieta, V. S., Ospina, J. H. G., Herrera Herrera, S., Ferney Rodríguez Rojas, C., and María Santis Navarro, A. (2024). Carbon dioxide emissions from traditional and modified concrete. A review. *Environ. Dev.* 52, 101036. doi:10.1016/j.envdev.2024.101036

Pobłocki, K., Pawlak, M., Drzeżdżon, J., Gawdzik, B., and Jacewicz, D. (2024). Clean production of geopolymers as an opportunity for sustainable development of the construction industry. *Sci. Total Environ.* 928, 172579. doi:10.1016/j.scitotenv.2024.172579

Pu, S., Duan, W., Zhu, Z., Wang, W., Zhang, C., Li, N., et al. (2022). Environmental behavior and engineering performance of self-developed silico-aluminophosphate geopolymer binder stabilized lead contaminated soil. *J. Clean. Prod.* 379, 134808. doi:10.1016/j.jclepro.2022.134808

Qiu, Z., Meng, Q., Liu, Y., and Ma, A. (2025). "Influence of stone content, relative density, and gradation on shear dilatancy characteristics of rock–soil mixtures," in *Marine georesources and geotechnology*, 1–16.

Ren, X., Wang, F., He, X., and Hu, X. (2024). Resistance and durability of fly ash based geopolymer for heavy metal immobilization: properties and mechanism. *RSC Adv.* 14 (18), 12580–12592. doi:10.1039/d4ra00617h

Sahoo, S., and Singh, S. P. (2022). Strength and durability properties of expansive soil treated with geopolymer and conventional stabilizers. *Constr. Build. Mater.* 328, 127078. doi:10.1016/j.conbuildmat.2022.127078

Shahedan, N. F., Hadibarata, T., Abdullah, M. M. A. B., Jusoh, M. N. H., Rahim, S. Z. A., Isia, I., et al. (2024). Potential of fly ash geopolymer concrete as repairing and retrofitting solutions for marine infrastructure: a review. *Case Stud. Constr. Mater.* 20, e03214. doi:10.1016/j.cscm.2024.e03214

Shivaprasad, K. N., Yang, H. M., and Singh, J. K. (2024). A path to carbon neutrality in construction: an overview of recent progress in recycled cement usage. *J. CO_2 Util.* 83, 102816. doi:10.1016/j.jcou.2024.102816

Song, S., Sohn, D., Jennings, H. M., and Mason, T. O. (2000). Hydration of alkali-activated ground granulated blast furnace slag. *J. Mater. Sci.* 35, 249–257. doi:10.1023/a:1004742027117

Song, Y., Xue, C., Guo, W., Bai, Y., Shi, Y., and Zhao, Q. (2024). Foamed geopolymer insulation materials: research progress on insulation performance and durability. *J. Clean. Prod.* 444, 140991. doi:10.1016/j.jclepro.2024.140991

Stavridakis, E. I. (1999). Influence of liquid limit and slaking on cement stabilized clayey admixtures. *Geotechnical and Geol. Eng.* 17, 145–154. doi:10.1023/A:1008953005726

Su, Y., Luo, B., Luo, Z., Xu, F., Huang, H., Long, Z., et al. (2023). Mechanical characteristics and solidification mechanism of slag/fly ash-based geopolymer and cement solidified organic clay: a comparative study. *J. Build. Eng.* 71, 106459. doi:10.1016/j.jobe.2023.106459

Sukprasert, S., Hoy, M., Horpibulsuk, S., Arulrajah, A., Rashid, A. S. A., and Nazir, R. (2021). Fly ash based geopolymer stabilisation of silty clay/blast furnace slag for subgrade applications. *Road Mater. Pavement Des.* 22 (2), 357–371. doi:10.1080/14680629.2019.1621190

Wang, J., Wu, L., and Feng, R. (2017). An experimental case study of a high-liquid-limit lateritic soil with its application in road construction. *Road Mater. Pavement Des.* 18 (6), 1423–1433. doi:10.1080/14680629.2016.1211031

Wang, X., Zhong, J., and Sun, Y. (2025). Innovative strategy to reduce autogenous shrinkage in alkali-activated slag using hydrophilic carbon nanotube sponge. *Compos. Part B Eng.* 299, 112447. doi:10.1016/j.compositesb.2025.112447

Wang, Z., Si-fa, X., and Guo-cai, W. (2012). Study of early strength and shrinkage properties of cement or lime solidified soil. *Energy Procedia* 16, 302–306. doi:10.1016/j.egypro.2012.01.050

Xie, J., Li, C., Li, B., Tang, J., and Gu, F. (2025). Thermal-alkaline activation enhances the mechanical properties of low-activity recycled concrete powder-derived geopolymers. *Constr. Build. Mater.* 463, 140020. doi:10.1016/j.conbuildmat.2025.140020

Xie, J., Zhang, J., Cao, Z., Blom, J., Vuye, C., and Gu, F. (2024). Feasibility of using building-related construction and demolition waste-derived geopolymer for subgrade soil stabilization. *J. Clean. Prod.* 450, 142001. doi:10.1016/j.jclepro.2024.142001

Yang, S., Yao, X., Li, J., Wang, X., Zhang, C., Wu, S., et al. (2021). Preparation and properties of ready-to-use low-density foamed concrete derived from industrial solid wastes. *Constr. Build. Mater.* 287, 122946. doi:10.1016/j.conbuildmat.2021.122946

Zhang, B. (2024). Durability of low-carbon geopolymer concrete: a critical review. *Sustain. Mater. Technol.* 40, e00882. doi:10.1016/j.susmat.2024.e00882

Zhang, M., Guo, H., El-Korchi, T., Zhang, G., and Tao, M. (2013). Experimental feasibility study of geopolymer as the next-generation soil stabilizer. *Constr. Build. Mater.* 47, 1468–1478. doi:10.1016/j.conbuildmat.2013.06.017